



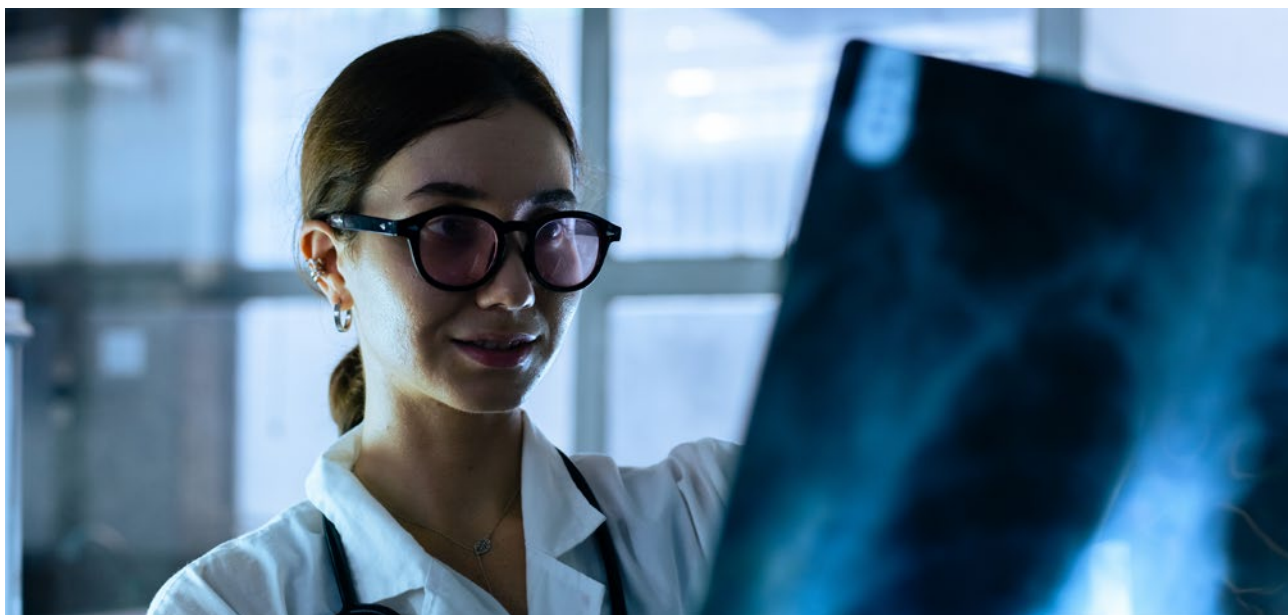
Abstract Highlights

The following highlights spotlight selected abstracts presented at the European Congress of Radiology (ECR) 2024. Covering a range of topics, from deep learning applications in neurological disorders to using a single cranial CT slice for identifying deceased individuals, these highlights present the latest cutting-edge developments in radiology.

Citation:

EMJ Radiol. 2024;5[1]:29-35.
<https://doi.org/10.33590/emjradiol/SEFB6923>.





A Comprehensive Approach to Reading Paediatric Chest X-rays

CHEST X-RAY is the most frequently ordered radiological investigation in paediatric health facilities; thus, errors in interpretation must be minimised. A systematic, comprehensive approach to reading paediatric chest X-rays, aimed at Paediatric and Radiology residents, was recently presented at ECR 2024, held from 28th February–3rd March in Vienna, Austria.

In this educational session, the authors emphasised that interpretation of paediatric chest X-rays is a taught skill that requires a multistep approach. Firstly, they highlighted some preliminary steps to follow, including checking the patient's clinical history, as this will be interrelated with the chest X-ray findings; and the patient's age, which is correlated with the presence or absence of the thymus, and the expected signs of bony maturity.

The authors also stressed the importance of recognising suboptimal technical factors, which may degrade the quality of chest X-rays, and lead to misinterpretations. For instance, they noted that poor inspiration is associated with

false cardiomegaly and diffuse opacification of the lungs, and a high degree of film rotation may lead to false hyperlucency of the lung, a pseudo mass, or false positive impression of cardiomegaly. Radiologist should aim for central positioning, where clavicles are symmetrically shaped, and the trachea is centrally positioned between the right and left pedicles.

The authors then detailed how to interpret a normal paediatric chest X-ray, by providing an analysis of eleven structures: the abdomen, diaphragm, costophrenic angle, chest wall soft tissue, bones, thymus, airway, heart, aorta, hila, and lungs. For each structure, they presented a checklist to aid in evaluation of the X-ray.

Finally, the study emphasised the common variants, and the unconventional appearance of normal structures, on a paediatric chest X-ray. The authors explained that this could be especially helpful for residents who are accustomed to reading adult chest X-rays, and are new to paediatric chest X-rays. ●

"In this educational session, the authors emphasised that interpretation of paediatric chest X-rays is a taught skill that requires a multistep approach."

The Broad Imaging Spectrum of Adenomyosis: Beyond the Junctional Zone Thickening

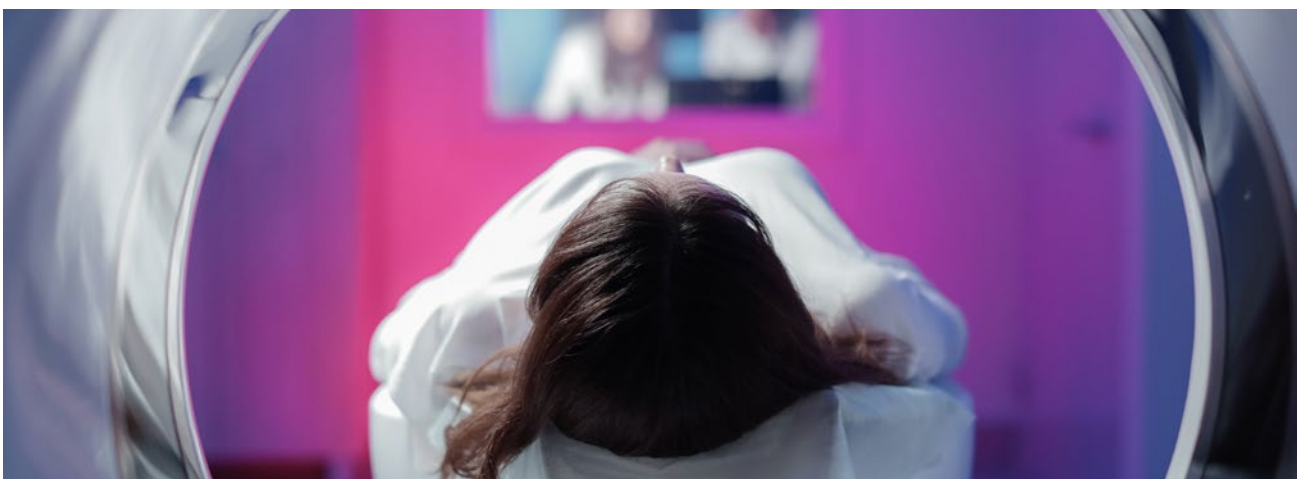
ADENOMYOSIS is a widespread benign gynaecological condition, in which the uterine lining penetrates the muscular wall of the uterus. Symptoms commonly include painful menstruation (dysmenorrhoea), chronic pelvic pain, and heavy bleeding during menstruation, known as menorrhagia. In new research presented at ECR 2024, held from 28th February–3rd March in Vienna, Austria, the highlights and pitfalls of MRI as a diagnostic tool for adenomyosis were explored.

As discussed in the session, the pathogenesis of adenomyosis is as follows: endometrial basalis cells will migrate and proliferate within the myometrium, forming an adenomyotic lesion. Alternatively, an ectopic endometrium will form by *de novo* metaplasia of stem cells, or implantation of stem cells through retrograde menstruation and invasion of the outer myometrium, known as 'outside-to-inside invasion'. MRI images the innermost layer in the myometrium, called the junctional zone (JZ), and the classification and subsequent reporting as internal or external adenomyosis was described. For instance, if JZ thickness is over 12 mm, it is classed as internal adenomyosis, whereas a thickness of less than 8 mm is external adenomyosis. The size of the affected area also determines classification as focal or diffuse.

Researchers emphasised how the pseudo-thickening of the JZ during the menstrual phase can sometimes lead to a misdiagnosis of adenomyosis, with the recommendation to avoid MRI scanning during this time. It was additionally stressed that whilst JZ thickness is generally a reliable marker for adenomyosis diagnosis, hormone conditions, such as pregnancy and pre-menarcheal age, can affect the JZ. The JZ also may not be measurable in approximately 30% of postmenopausal uteruses, and in females using contraceptive drugs. It was additionally noted that several other benign conditions and malignant tumours have also shown to exhibit similar JZ characteristics to adenomyosis, such as uterine and JZ enlargement. Conditions mentioned included lymphoma, low-grade endometrial stromal sarcoma, myometrial involvement by pelvic endometriosis, and transient myometrial contraction.

The study concluded that adenomyosis can be accurately diagnosed by using MRI; however, it is imperative to be aware of both the typical and atypical features of adenomyosis, as well as other possible conditions that exhibit a similar phenotype. ●

"Pseudo-thickening of the JZ during the menstrual phase can sometimes lead to a misdiagnosis of adenomyosis."



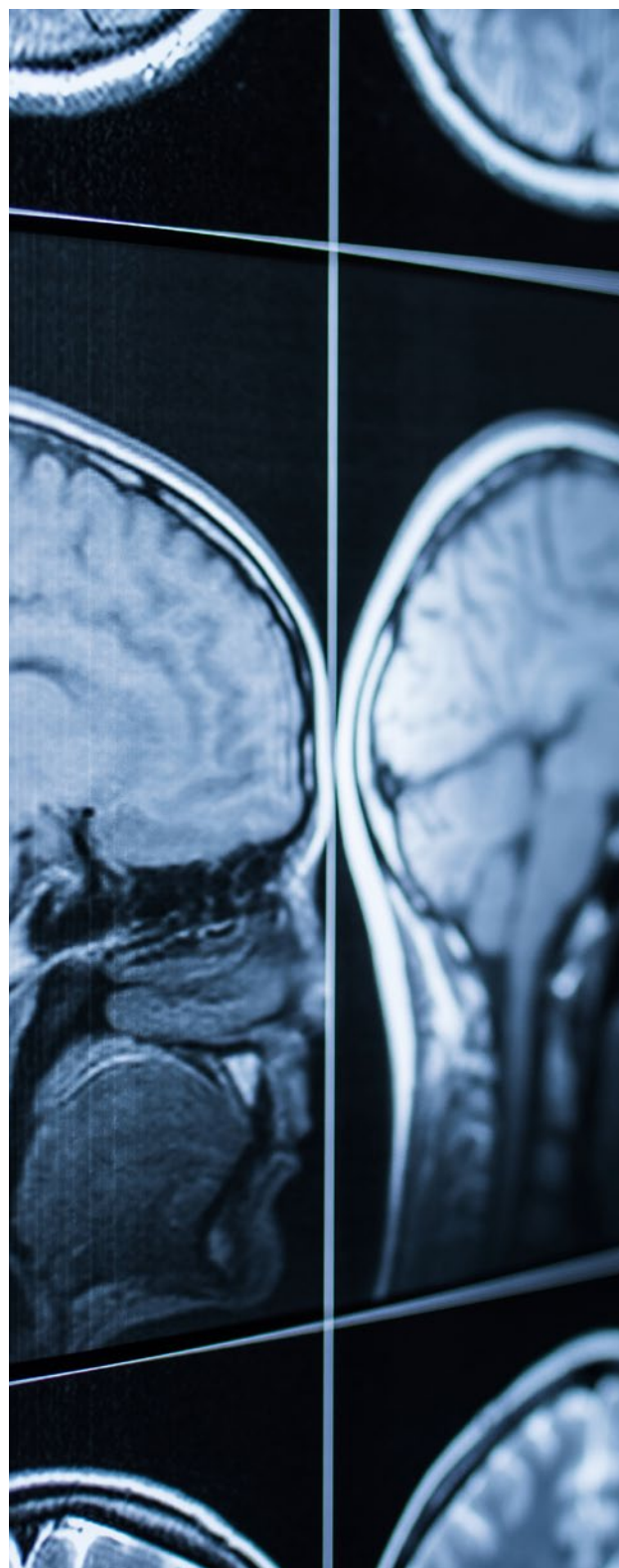
Deep Learning Applications for Alzheimer's Disease

ALGORITHMS based on deep learning, with applications for diagnosis, developing prediction models, and treatment research, were outlined in an abstract presented at ECR 2024. The abstract was intended to inform neuroimaging prediction in radiologists.

Dementia affects over 55 million people worldwide, and as the seventh global cause of death, approximately 65% of cases are attributable to Alzheimer's disease (AD). The significant burden this has on patients, caretakers, and the economy is vast, but emerging research aims to combat the progressive decline in cognition, and severe impairment caused by the condition. Early intervention can delay this decline, and improve quality of life. Modern neuroimaging techniques, aided by emerging AI and deep learning models, allow rapid and accurate assessment of key markers, such as brain atrophy, the accumulation of neurotoxic proteins, and synaptic disruptions.

The emergence of these AI and deep learning-guided algorithms has provided solutions for semi-automated and automated brain segmentation and morphometry. Highly detailed reports are used, and a novel tool for AD detection and mild cognitive impairment prognostic has been developed, relying on lifespan trajectories of brain structures. This Hippocampal-Amygdalo-Ventricular Alzheimer score (HAVAs) is based on lifespan models of normal population, and patients with AD. After validation, it has shown great capability in detecting patients with AD, compared to control subjects. The probability score has shown considerable accuracy, both in diagnosis and prognosis.

From this abstract, and the other research shared at ECR 2024, it is clear that AI-based solutions are rapidly finding their way into AD clinical practice, and are set to improve patients' quality of life dramatically. Neuroimaging plays a key role in the diagnosis and monitoring of AD, and the new software outlined provides automated and time-saving solutions, which will significantly aid neuroradiologists in identifying disease earlier, staging this, and monitoring both evolution and treatment response. ●



"AI and deep learning models allow rapid and accurate assessment of key markers."

Videofluoroscopic Swallow Study in Diagnosing Dysphagia

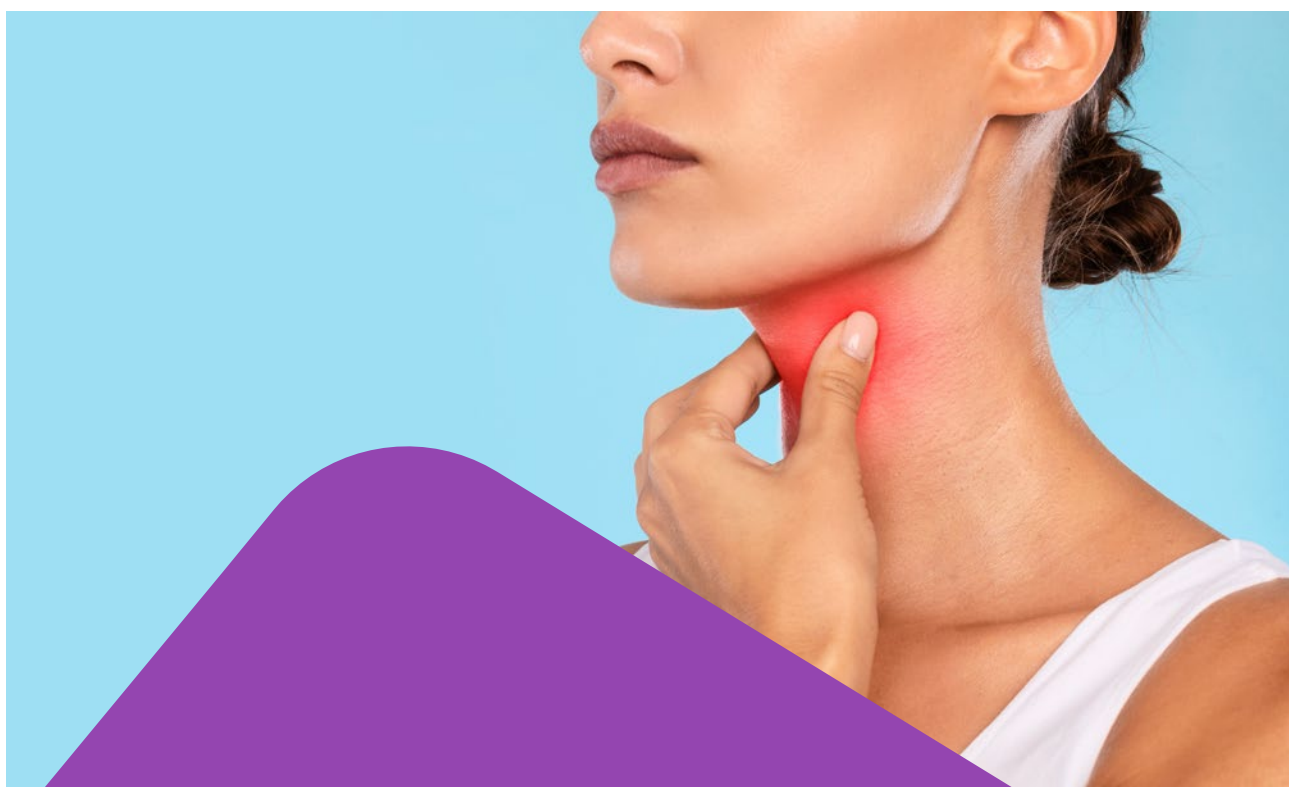
DYSPHAGIA, a debilitating condition, can lead to severe complications, including malnutrition, dehydration, aspiration pneumonia, and even death. Dysphagia is commonly a result of various medical conditions and their associated treatment complications, with prevalence increasing with age. Research presented at ECR 2024 explored the diagnosis of this condition.

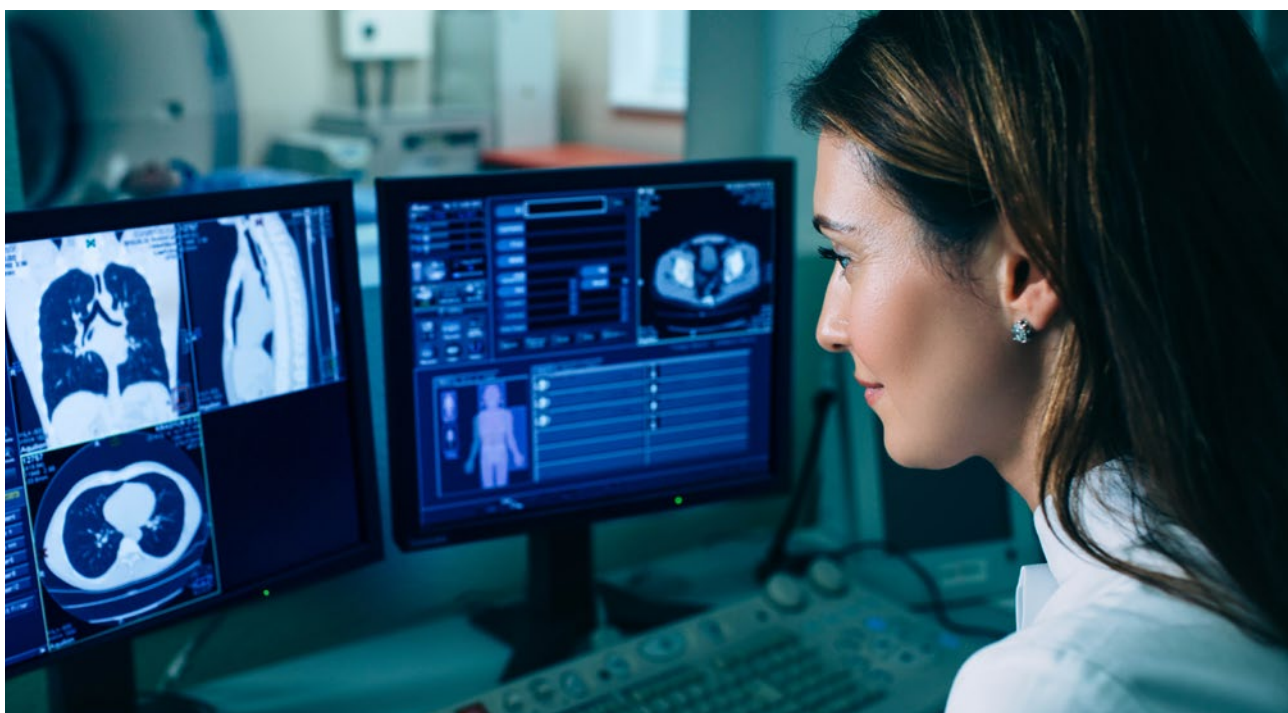
The gold standard investigation for diagnosing dysphagia is the videofluoroscopic swallow study (VFSS), a dynamic fluoroscopic study. VFSS is often performed by collaboration between speech therapists and radiologists, and through the use of fluoroscopy, clinicians can visualise bolus flow through the aerodigestive tract in relation to structural changes. Overall, this enables real-time evaluation of the patient's swallowing physiology, specifically enabling the detection of any penetration/aspiration, underlying functional and/or structural abnormalities, and the observation of the effects of different bolus consistencies/volumes on swallowing.

Commonly, patients present with a combination of swallowing pathologies across different phases of swallowing. However, these pathologies may be difficult to identify, as swallowing occurs rapidly in real-time. Viewing these pathologies in slow motion is helpful to ensure abnormalities are not missed, and enables the identification of subsequent individualised rehabilitative therapy.

"VFSS is often performed by collaboration between speech therapists and radiologists."

VFSS allows the comprehensive assessment of oropharyngeal dysphagia and risk of aspiration, and is a useful tool in providing a preliminary evaluation of oesophageal motility. A good understanding of swallow physiology is important in identifying the underlying cause of dysphagia, before also guiding rehabilitation and management. ●





Advantages of Photon-Counting CT

PHOTON-COUNTING CT is an emerging imaging technique that promises a vast array of advantages for radiologists, as explored in new research presented at ECR 2024, held from 28th February–3rd March in Vienna, Austria.

Conventional CT, despite its widespread use and availability, continues to struggle with challenges in radiation exposure, image noise, and limited tissue differentiation, according to the study's authors. Photon-counting CT may be the solution to many of these issues, with the potential for enhanced spatial resolution, reduced radiation noise, and improved characterisation of tissues. This new technology promises success, as photon-counting detectors (PCD) consist of a single layer of a semiconductor diode with applied voltage, and therefore do not need a separate layer to convert X-rays into light in the way of energy-integrating detectors. In a PCD, the authors explained, an X-ray is absorbed, generating positive and negative charges separated rapidly, and creating an electrical pulse in attached wires, which is then registered by an electronic readout circuit.

As a result of its unique operating method, photon-counting CT provides several clinical benefits to radiographers. This emerging

technology may improve the ways in which cardiac imaging is performed, increasing spatial resolution in coronary angiography, and reducing radiation noise in cardiac CT imaging. The authors went on to describe the ways in which photon-counting CT may also improve neuroimaging, and tumour detection and imaging, particularly when applied to small tumours and lesions.

"This emerging technology may improve the ways in which cardiac imaging is performed."

The study concluded that photon-counting CT has the potential to surpass conventional CT, as it provides improved spatial resolution, noise elimination, and efficient dose usage. PCD additionally may benefit larger patients, as it addresses artifacts like calcium blooming. Photon-counting CT has a wide range of applications in various areas of medicine, and therefore provides a promising future for radiography. ●

Identifying Deceased Individuals Using Single Cranial CT Slice

AUTOMATIC identification of unknown deceased individuals has been achieved with single cranial CT (CCT) slices, using a novel computer vision (CV)-based method. This research was presented at ECR 2024.

Orthopantomograms (OPG) are often used in the identification of unknown persons; however, these are difficult to acquire post-mortem. As such, CT is the preferred post-mortem imaging modality. Considering the lack of literature exploring the use of CCT imaging to identify deceased individuals, researchers extended an automatic CV-based identification method used to extract CV features from OPGs to individual CCT images.

Using OPGs as a reference, a total of 819 CCT scans from 772 individuals aged between 10–99 years (321 females; 452 males; and 46 unknown), obtained between November 2016–May 2023, were retrospectively analysed across six defined regions: lower row of teeth, upper row of teeth, end of maxilla, cervical spine, maximal representation of maxillary sinus, and maximal representation of eye structures.

In instances where large metal or movement artifacts were present, accurate location of these six regions was not achievable, and thus, specific images for these areas could not be exported to aid identification. Subsequently, a further 1,771 OPGs from these individuals between December 2000–May 2023 were included. CV features were extracted from imaging using the AKAZE algorithm.

To enable individual identification, 50–69 CT slices per region from individuals with at least two examinations were compared with up to 818 database entries, and a further 410 OPGs were matched with 1,759 OPGs from the same individuals. Following this, calculation of a CV feature matching concordance metric was performed (matching points/number of key points) [%]).

"The highest success was seen in the maxillary sinus region."

Identification was achieved for 72–87% (rank: 1–10) of the identities using CT images. Same-individual identification across all six CT regions achieved a concordance metric score of $12.04 \pm 0.86\%$, compared to $2.15 \pm 0.40\%$ for different individuals. This difference could be a result of metal artifacts or lower image resolution. The highest success was seen in the maxillary sinus region, with identification rates of 72%, 80%, and 87% for rank 1, 5, and 10, respectively.

The study concluded that a single CCT slice can be used to identify unknown individuals, and that future research assessing CT abdomen and thorax imaging for other distinctive CV features to further improve identification success rates, should be explored. ●

